

Potassium-doped Co_3O_4 catalyst for direct decomposition of N_2O

Kimihiro Asano ^a, Chie Ohnishi ^a, Shinji Iwamoto ^a,
Yasushi Shioya ^b, Masashi Inoue ^{a,*}

^a Department of Energy and Hydrocarbon Chemistry, Graduate School of Engineering,
Kyoto University, Katsura, Kyoto 615-8510, Japan

^b Süd-Chemie Catalysts Japan Inc., 635 Sasakura, Fuchu, Toyama 939-2753, Japan

Received 24 March 2007; received in revised form 13 September 2007; accepted 16 September 2007

Available online 19 September 2007

Abstract

Direct decomposition of nitrous oxide (N_2O) on K-doped Co_3O_4 catalysts was examined. The K-doped Co_3O_4 catalyst showed a high activity even in the presence of water. In the durability test of the K-doped Co_3O_4 catalyst, the activity was maintained at least for 12 h. It was found that the activity of the K-doped Co_3O_4 catalyst strongly depended on the amount of K in the catalyst. In order to reveal the role of the K component on the catalytic activity, the catalyst was characterized by XRD, XPS, TPR and TPD. The results suggested that regeneration of the Co^{2+} species from the Co^{3+} species formed by oxidation of Co^{2+} with the oxygen atoms formed by N_2O decomposition was promoted by the addition of K to the Co_3O_4 catalyst.

© 2007 Elsevier B.V. All rights reserved.

Keywords: N_2O decomposition; Co_3O_4 catalyst; Alkali promoting effect; Redox mechanism

1. Introduction

Nitrous oxide (N_2O) has a high global warming potential, 310 times larger than that of CO_2 [1], and contributes to the destruction of the ozone layer in the stratosphere [2]. It is emitted from both natural and anthropogenic sources such as nitric acid and adipic acid plants and fluidized bed combustors for sewage-sludge or industrial wastes [3] besides the medical exhaust and biological and agricultural emissions. The concentration of nitrous oxide in the atmosphere continues to increase, and this increase appears to be caused mainly by human activities. With increasing concerns about protecting our environment, the catalytic removal of nitrous oxide from exhausts becomes very attractive.

It was reported that nitrous oxide is easily decomposed to nitrogen and oxygen on various types of catalysts such as noble metals [2–5], metal oxides [6–10], and ion-exchanged zeolites [11–13]. However, few of them have been found to be active and stable enough for practical applications, because their activities are severely inhibited by the presence of other gases

such as O_2 . Moreover, oxygen atoms formed by the decomposition of nitrous oxide are hardly desorbed from the catalyst surface and accumulated on the surface, finally causing catalyst deactivation [3,14].

In the previous work, we have made a survey of various metal oxide catalysts for direct decomposition of nitrous oxide in the presence of oxygen in the feed, and found that the Co_3O_4 catalyst prepared by the precipitation method had a fairly high activity [15]. Then, we examined effect of the precipitation agent on the catalyst activity and found that when NaHCO_3 was used as a precipitation agent, CoCO_3 was precipitated as a precursor, calcination of which gave a catalyst having quite a high activity. We also found that the activity of the catalyst depended on the amount of alkali and alkaline earth metals remaining in the catalyst [16]. Since CoCO_3 particles are negatively charged, alkali cations are adsorbed on the surface of the precursor, and the catalyst prepared from this precursor had a suitable alkali content. Therefore, effect of alkali doping on CoCO_3 was examined, and the adequate amount of Na added to the Co catalyst was found to be $\text{Na/Co} = 3.8 \times 10^{-3}$. As for direct decomposition of NO, Park et al. [17] reported that alkali-promoted Co_3O_4 catalyst had high activity. Haneda et al. [18] also reported a similar result and concluded that potassium was the most effective additive for the Co_3O_4 catalyst. They

* Corresponding author. Tel.: +81 75 383 2478; fax: +81 75 383 2479.

E-mail address: inoue@scl.kyoto-u.ac.jp (M. Inoue).

found that the addition of O_2 to the feed caused a significant decrease in the activity of the catalyst for direct decomposition of NO .

In the present paper, K-doped Co_3O_4 catalysts were prepared by impregnation of KNO_3 on $CoCO_3$ because the alkali content can be finely tuned. We report the performance of the catalysts for N_2O decomposition and reveal the role of the K component on the activity of the Co_3O_4 catalyst on the basis of characterization of the catalyst.

2. Experimental

2.1. Preparation of Co_3O_4 catalyst

Catalysts were prepared by an impregnation method. Potassium was doped to $CoCO_3$ with an aqueous solution of KNO_3 , followed by drying at $80^\circ C$. The atomic ratio of potassium to Co_3O_4 (K/Co) was varied from 0 to 0.1. The Co_3O_4 catalyst was prepared by calcinations at $400^\circ C$ for 4 h in air.

2.2. Catalytic activity test

Catalyst tests were carried out in a fixed-bed flow reactor. The catalyst was tabletted, pulverized into 10–22 mesh, and set in the reactor. The catalyst bed was heated to $500^\circ C$ in a helium gas flow and held at that temperature for 30 min. Then, the reaction gas composed of 5000 ppm N_2O , 2% O_2 , 0 or 2.5% H_2O , and He balance was introduced to the catalyst bed at $W/F = 0.3 \text{ g s ml}^{-1}$. Although N_2O decomposition is highly exothermic (-82.05 kJ/mol), the feed gas contain only 5000 ppm N_2O and no temperature jump was recognized at the onset of the reaction since the heat capacities of the catalyst bed and the reactor were large enough. The effluent gases from the reactor were analyzed every 5 min at $500^\circ C$ with an on-line micro-gas-chromatograph (CP 2002, Chrompack, Netherlands) (columns: 10 m Molecular Sieve 5A at $80^\circ C$; 10 m Porapack Q at $40^\circ C$). After the steady state was attained, reaction temperature was decreased from $500^\circ C$ to the temperature where the catalyst showed negligible N_2O conversion. The catalyst activity is expressed by the T_{50} value, which is defined as the temperature at which the catalyst Exhibits 50% N_2O conversion under the above-mentioned conditions.

2.3. Characterization

Powder X-ray diffraction (XRD) pattern were recorded on a Shimadzu XD-D1 diffractometer using $Cu K\alpha$ radiation and a carbon monochromator. Thermogravimetric (TG) analysis was performed on a Shimadzu DTG-50 analyzer at a heating rate of $10^\circ C/\text{min}$ in a 40 ml/min flow of dried air. The specific surface area was calculated using the BET single-point method from nitrogen uptake measured at 77 K. The samples were pretreated in an N_2 flow at $300^\circ C$ for 30 min prior to the measurements. Reduction behavior of the catalyst was examined by temperature-programmed reduction with H_2 (H_2 -TPR). A portion (0.01 g) of a sample was set in a reactor, activated at $600^\circ C$ for 1 h in an Ar flow and cooled to room temperature. A

gas mixture (2 vol% H_2 -Ar) was introduced to the reactor at a flow rate of 20 ml/min and the sample was heated at a rate of $5^\circ C/\text{min}$ till $900^\circ C$. The hydrogen content in the effluent gas from the reactor was measured by a TCD detector of a Shimadzu GC-4C gas chromatograph. The XPS measurements were carried out with an ULVAC-PHI model 5500 spectrometer with 15 kV, 400 W $Mg K\alpha$ emission as the X-ray source. The binding energy was corrected by the contaminated carbon (284.6 eV). Temperature-programmed desorption (TPD) of O_2 and N_2O was also carried out in the fixed-bed flow reactor. The pretreatment conditions were the same as in the case of the catalyst tests ($500^\circ C$, 30 min in He). After the heat treatment in the helium flow, the temperature of the catalyst bed was decreased to $50^\circ C$. The gas composed of 2% O_2 or 5000 ppm N_2O with the balance helium was introduced into the catalyst bed at $W/F = 0.3 \text{ g s ml}^{-1}$, kept flowing for 1 h, and then purged in He (100 ml/min) for 1 h. After the treatment, the temperature was raised to $600^\circ C$ at a rate of $5^\circ C/\text{min}$ in the helium flow (100 ml/min), and the effluent gases from the reactor were analyzed with a Pfeiffer Vacuum Omnistar GSD 301 O 1 quadrupole mass spectrometer.

3. Results and discussion

3.1. N_2O decomposition over K-doped Co_3O_4 catalysts

The activities of the catalysts with different K/Co molar ratios for N_2O decomposition are shown in Fig. 1. The activity of the undoped Co_3O_4 catalyst was low and N_2O conversion of the Co_3O_4 catalyst at $300^\circ C$ was less than 10%. The addition of a small amount of K (K/Co = 0.01) drastically enhanced the activity of the Co_3O_4 catalyst for N_2O decomposition, and N_2O conversion of the K-doped Co_3O_4 catalysts at $300^\circ C$ were over 80%. The results for N_2O decomposition under wet conditions are shown in Fig. 2. The presence of water in the feed drastically decreased the catalyst activity, and N_2O conversion

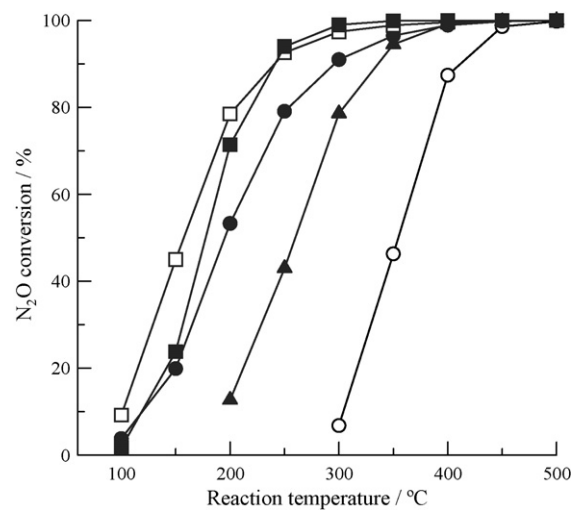


Fig. 1. N_2O decomposition activities of Co_3O_4 catalysts. Reaction conditions: N_2O , 5000 ppm; O_2 , 2%; He balance; $W/F = 0.3 \text{ g s ml}^{-1}$. K-doped Co_3O_4 catalysts with K/Co molar ratios of: \bigcirc , 0 (Co_3O_4); \bullet , 0.01; \square , 0.02; \blacksquare , 0.05; \blacktriangle , 0.10.

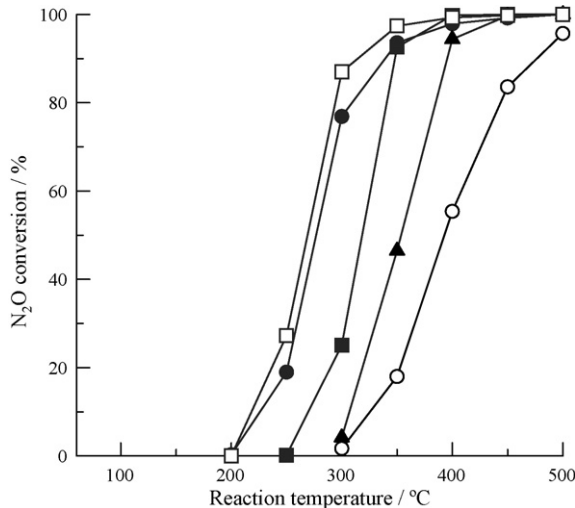


Fig. 2. N_2O decomposition activities of Co_3O_4 catalysts. Reaction conditions: N_2O , 5000 ppm; O_2 , 2%; H_2O , 2.5%; He balance; $\text{W/F} = 0.3 \text{ g s ml}^{-1}$. K-doped Co_3O_4 catalysts with K/Co molar ratios of: ○, 0 (Co_3O_4); ●, 0.01; □, 0.02; ■, 0.05; ▲, 0.10.

at 200 °C was negligible. This result suggests that water is adsorbed on the active sites disturbing the catalytic activity. Fig. 3 shows the dependence of the activity of the K-doped Co_3O_4 catalyst on the K/Co molar ratio. Under the dry conditions, the activity increased as the K/Co molar ratio increased, and the catalyst with K/Co molar ratio of 0.03 showed the highest activity. Further increase in the K/Co molar ratio resulted in a decrease in the activity. This tendency was maintained under the wet conditions, although the N_2O conversion under the wet conditions was lower than that under the dry conditions, irrespective of the K/Co ratio. The highest activity was attained by the catalyst with the K/Co molar ratio of 0.02. These optimal M/Co ratios were essentially identical with those reported by Park et al. [17] (0.015) and Haneda et al.

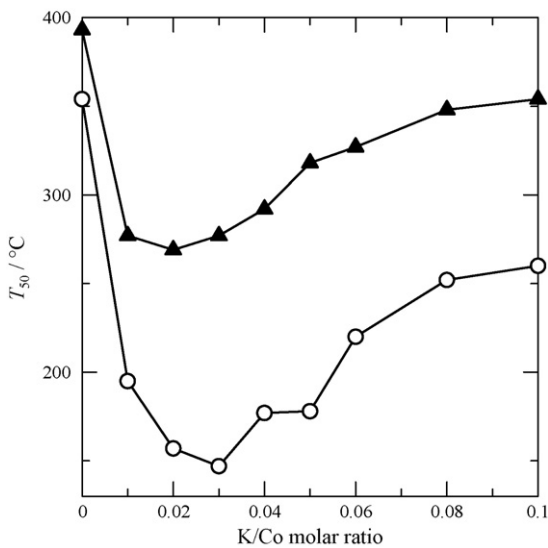


Fig. 3. Temperature of 50% N_2O conversion (T_{50}) vs. K/Co molar ratio. Reaction conditions: N_2O , 5000 ppm; O_2 , 2%; H_2O , 0 or 2.5%; He balance; $\text{W/F} = 0.3 \text{ g s ml}^{-1}$. ○, without H_2O ; ▲, with H_2O .

[18] (0.035 for potassium) for direct decomposition of NO , suggesting that these two reactions (decomposition of N_2O examined in this work and decomposition of NO) take place on the same active sites of the catalysts. Slight difference in the optimal ratios may be due to the difference in the catalyst preparation methods: Park et al. [17] and Haneda et al. [18] adopted impregnation of Co_3O_4 with alkali nitrate solutions while the catalysts were prepared by impregnation of CoCO_3 with a potassium nitrate solution and subsequent calcination in the present work. The latter procedure was adopted because we found that it gave the catalysts having higher activity than those prepared by the former procedure [15,16].

The BET surface area of the K-doped Co_3O_4 catalyst varied with the K/Co molar ratio as shown in Fig. 4. With increasing the K/Co molar ratio, the BET surface area increased, and the largest BET surface area was attained by the K/Co molar ratio of 0.06. This result indicates that the development of the Co_3O_4 crystals by decomposition of CoCO_3 was somehow prevented by the presence of K ions. However, the activity of the K-doped Co_3O_4 catalyst for N_2O decomposition does not depend on the BET surface area; for example, with the addition of a small amount of K ($\text{K/Co} = 0.01$), the activity of the catalyst for N_2O decomposition drastically improved, but the BET surface area did not improve much.

Catalytic durability under the dry and wet conditions was examined, and the results are shown in Fig. 5. The K-doped Co_3O_4 catalyst maintained over 80% N_2O conversion at least for 12 h even in the presence of 2.5% water in the feed gas. In the figure, the data obtained by the experiment carried out in the absence of oxygen under the dry condition are also given. The absence of O_2 in the feed increased the N_2O conversion and the catalyst maintained high N_2O conversion level at least for 6 h. Therefore, the presence of O_2 in the feed does not have any effect on the long-term activity of the catalyst. To examine possible leaching of the alkali component, the catalyst compositions before and after the duration test were examined. However, the molar ratio of K/Co of the used catalyst

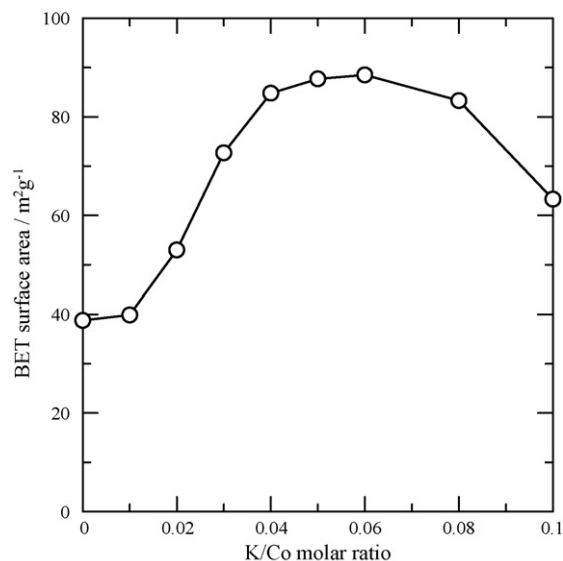


Fig. 4. BET surface areas of K-doped Co_3O_4 catalysts.

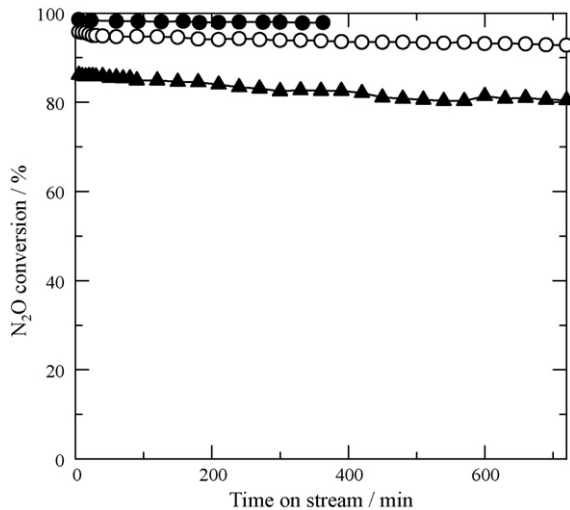


Fig. 5. Durability tests at 300 °C of the Co_3O_4 catalyst with K/Co molar ratio of 0.02. Reaction conditions: N_2O , 5000 ppm; O_2 , 2%; H_2O , 0 or 2.5%; He balance; $\text{W/F} = 0.3 \text{ g s ml}^{-1}$. \circ , without H_2O ; \blacktriangle , with H_2O . For comparison, data obtained with the feed gas of 5000 ppm of N_2O without O_2 or H_2O are given by closed-circle marks.

determined by ICP was identical with that found in the fresh catalyst (K/Co = 0.021).

Some catalysts are known to have high activities for N_2O decomposition, and the Rh catalyst was reported to decompose N_2O even at room temperature; however, because the oxygen atoms formed by N_2O decomposition remained on the catalyst surface, the activity of the Rh catalyst abruptly decreased after maintaining high activity for a while [19,20]. Moreover, it was reported that the catalyst was promptly deactivated when oxygen was present in the feed [20]. In the case of the K-doped Co_3O_4 catalyst, high activity was maintained for more than 12 h, even in the presence of oxygen. This result suggests that oxygen formed by the decomposition of N_2O is easily desorbed from the surface of the present catalyst.

3.2. XRD patterns of the catalysts

Fig. 6 shows the XRD patterns of the K-doped Co_3O_4 catalysts prepared. All the XRD peaks were attributed to the spinel structure, indicating that no other crystalline phases than Co_3O_4 were formed. The peaks became broader by the addition of K ions but the peak shift was not observed, indicating that K ions are highly dispersed in the matrix of the Co_3O_4 catalyst.

3.3. Thermal analysis of the precursors

Fig. 7 shows the TG profiles of the precursors, all of which showed essentially the same profile, and two weight decrease processes were observed at the temperature ranges of 200–250 °C and ~900 °C. The former weight decrease is due to decomposition of the precursor, CoCO_3 , releasing CO_2 and subsequent oxidation of CoO into Co_3O_4 , and the latter weight decrease is attributed to thermal reduction of Co_3O_4 to CoO releasing O_2 into the gas phase [21,22]. These results indicate that the impregnation of CoCO_3 with a KNO_3 solution has no

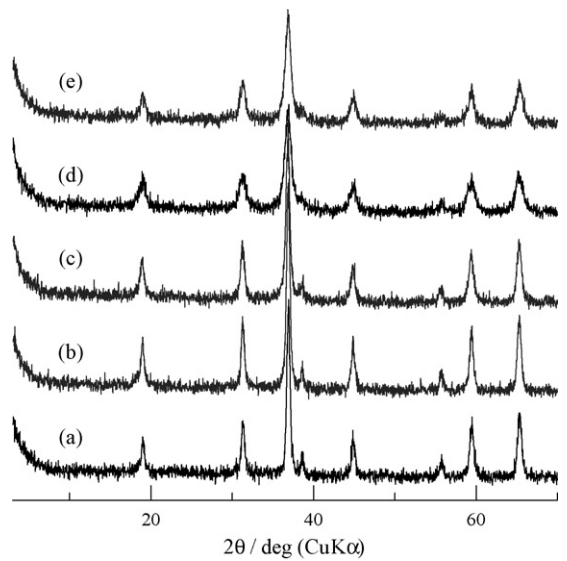


Fig. 6. XRD patterns of K-doped Co_3O_4 catalysts with K/Co molar ratios of: (a), 0 (Co_3O_4); (b), 0.01; (c), 0.02; (d), 0.05; (e), 0.10.

effect on the thermal decomposition behavior of CoCO_3 . The weight decrease observed at the temperature ranges of 700–800 °C for the K-doped Co_3O_4 catalyst with K/Co molar ratio of 0.10, is attributed to decomposition of KNO_3 .

3.4. Surface information of the K-doped Co_3O_4 catalyst obtained by XPS

Fig. 8 shows the Co 2p spectra observed for the catalysts with various K/Co molar ratios. For the undoped Co_3O_4 catalyst, the peak due to $\text{Co } 2p_{3/2}$ was observed at binding energy (BE) of 779.8 eV and this value was in good agreement with the reported data for Co_3O_4 [23,24]. However, the $\text{Co } 2p_{3/2}$ peak slightly shifted toward the lower BE side by the addition of a small amount of K, indicating a change in the electronic state

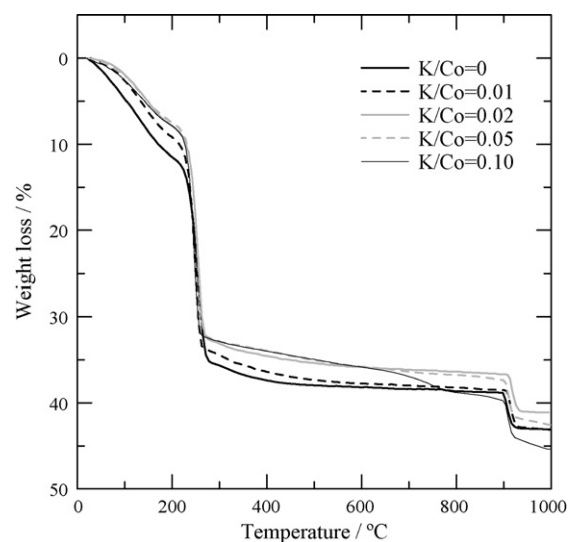


Fig. 7. Thermal decomposition behavior of the precursors.

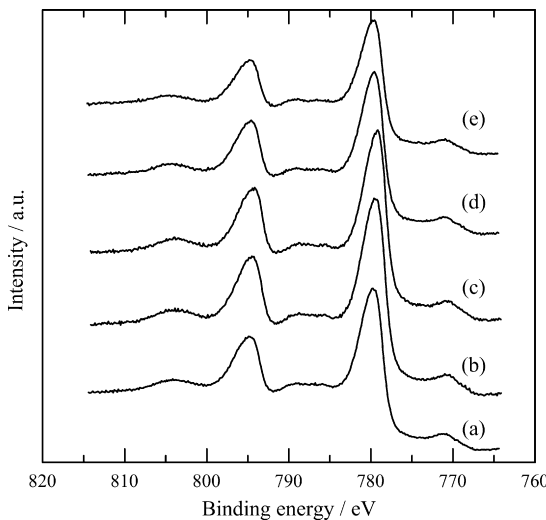


Fig. 8. Co 2p spectra of K-doped Co_3O_4 catalysts with K/Co molar ratios of: (a), 0 (Co_3O_4); (b), 0.01; (c), 0.02; (d), 0.05; (e), 0.10.

of cobalt to the lower valence side. Similar results have been reported [24] but explanation for these results may be different from those given by other researchers. Small amounts of potassium ions can be adsorbed on the particles to compensate the negative charge of the particles. Alkali cations are Lewis acids and have no electron donation effects. However, oxygen anions in the coordination sphere of the cations are highly basic and therefore electron donation from highly basic oxygen anions surrounding the alkali cation toward cobalt ion increases the electron density of cobalt ions and plays an important role in N_2O decomposition.

Fig. 9 shows the O 1s spectra of the catalysts. The peak at 529.0–529.5 eV is attributed to the O^{2-} anions of the crystalline network [23]. The O 1s peak slightly shifted toward the lower BE side by the addition of a small amount of K, indicating that the electronic density of oxygen increased (i.e., the basicity of oxygen anion became high.) Further addition of the K

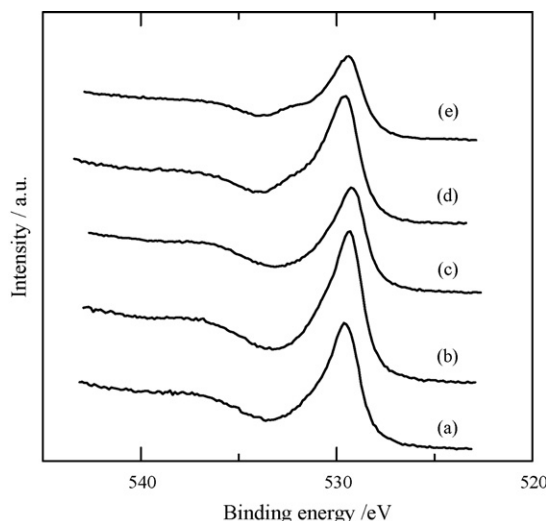


Fig. 9. O 1s spectra of K-doped Co_3O_4 catalysts with K/Co molar ratios of: (a), 0 (Co_3O_4); (b), 0.01; (c), 0.02; (d), 0.05; (e), 0.10.

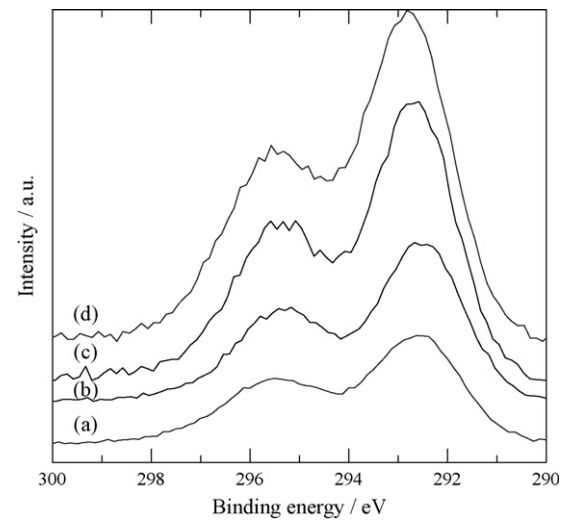


Fig. 10. K 2p spectra of K-doped Co_3O_4 catalysts with K/Co molar ratios of: (a), 0.01; (b), 0.02; (c), 0.05; (d), 0.10.

component caused higher BE shift. This shift may be due to the contribution of surface hydroxyl group bound to either cobalt or potassium ion.

Fig. 10 shows the K 2p spectra, the intensity of which became gradually larger with increasing the K/Co molar ratio. The main sharp line at 292.5–292.8 eV is due to $2\text{p}_{3/2}$ and the satellite line at 295.5 eV is attributed to $2\text{p}_{1/2}$ of potassium ion [25,26]. Relatively low BE of K 2p suggests that the counter anion of potassium ion is oxide anion (O^{2-}) [27], which further indicates that potassium ions strongly interact with the lattice oxygen of Co_3O_4 . The K $2\text{p}_{3/2}$ peak slightly shifted toward the higher BE side with increasing the K loading, showing a change in the electronic state of potassium. This result suggests that the contribution of hydroxide ion becomes significant for the catalyst with excess K loading, since KOH is known to exhibit higher BE [25,27].

Table 1 shows the K/Co atomic ratios determined by XPS, which were much greater than those adopted for preparation. This means that a lot of potassium ions are present in the surface region of the catalyst.

3.5. Reduction behavior of the K-doped Co_3O_4 catalyst

Fig. 11 shows the H_2 -TPR profiles of the K-doped Co_3O_4 catalysts. All the catalysts exhibited similar TPR profiles, and

Table 1
XPS results for K-doped Co_3O_4 catalysts

| Catalyst (K/Co molar ratio) | Binding energy (eV) | | Surface composition K/Co |
|-----------------------------------|----------------------|---------------------|--------------------------------|
| | Co 2p _{3/2} | K 2p _{3/2} | |
| Co_3O_4 (0) | 779.8 | – | – |
| K/ Co_3O_4 (0.01) | 779.6 | 292.6 | 0.0725 |
| K/ Co_3O_4 (0.02) | 779.2 | 292.7 | 0.104 |
| K/ Co_3O_4 (0.05) | 779.6 | 292.6 | 0.223 |
| K/ Co_3O_4 (0.10) | 779.6 | 292.8 | 0.321 |

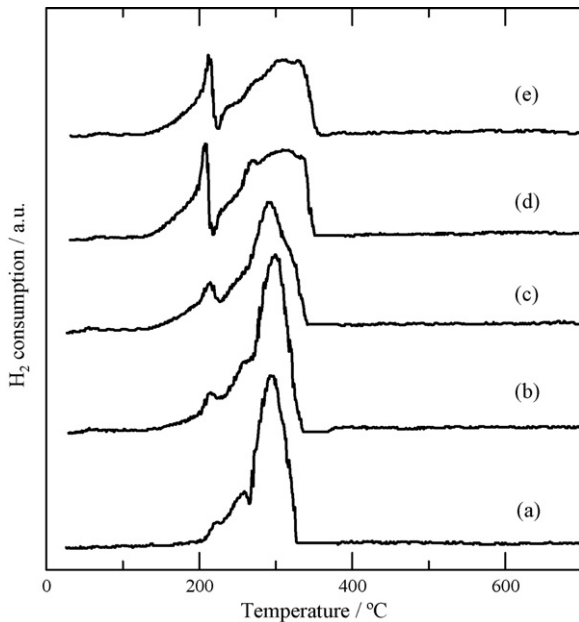


Fig. 11. TPR profiles of K-doped Co_3O_4 catalysts with K/Co molar ratios of: (a), 0 (Co_3O_4); (b), 0.01; (c), 0.02; (d), 0.05; (e), 0.10. Reaction condition: H_2 , 2%; Ar balance; W/F = 0.03 g s ml^{-1} . Heating rate; 5 $^{\circ}\text{C min}^{-1}$.

the reduction peaks were observed at around 200–300 $^{\circ}\text{C}$ and 300–400 $^{\circ}\text{C}$. The former peak was attributed to the reduction from Co^{3+} to Co^{2+} [28–31], and shifted toward low temperature by the addition of K. The latter peak was attributed to the reduction from Co^{2+} to metallic Co [28–31] and became broader with increasing the K content. These results suggest that interaction between K species and Co_3O_4 promoted the reduction of Co^{3+} to Co^{2+} . It is reasonable to assume that Co^{2+} is oxidized to Co^{3+} by the oxygen atom formed by the decomposition of N_2O . Then, the thus-formed Co^{3+} must be reduced to Co^{2+} to regenerate the active sites. The K species in the catalyst seems to play an important role in promoting this reduction step.

3.6. Temperature-programmed desorption

Temperature-programmed desorption of O_2 and N_2O were performed to understand the role of K ions in the N_2O decomposition process. Fig. 12 shows the oxygen desorption profiles for the catalysts. For the undoped Co_3O_4 catalyst, desorption peaks were observed at around 70–200 $^{\circ}\text{C}$, 250–350 $^{\circ}\text{C}$, and around 500 $^{\circ}\text{C}$. Addition of a small amount of K caused a significant change of the profile and the desorption peaks were apparently shifted toward lower temperatures. This result indicates that desorption of oxygen is promoted by the addition of K to Co_3O_4 . The largest intensity of the desorption peak was observed for the K-doped Co_3O_4 catalyst with K/Co molar ratio of 0.02, indicating that the number of oxygen adsorption sites correlates with the activity of the K-doped Co_3O_4 catalyst: The K-doped Co_3O_4 catalyst with higher activity for N_2O decomposition adsorbs more oxygen. Since the desorption of oxygen from the K-doped Co_3O_4 completed well below 180 $^{\circ}\text{C}$, the activity of the catalyst at 300 $^{\circ}\text{C}$ maintained

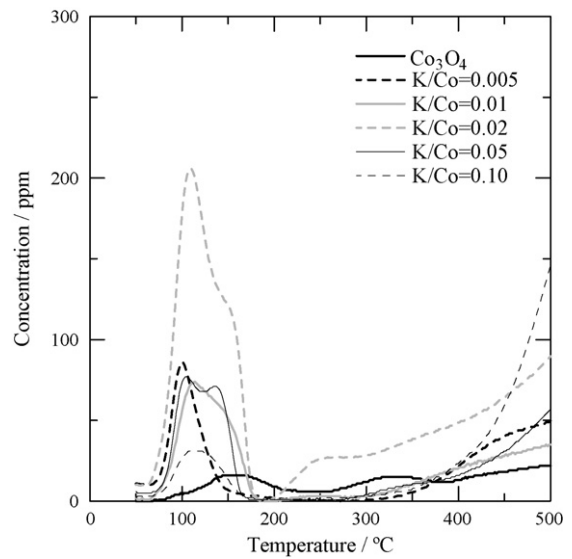


Fig. 12. O_2 -TPD profiles of K-doped Co_3O_4 catalysts.

at least for 12 h even in the presence of 2% oxygen in the feed gas.

The desorption profiles for preadsorbed N_2O on the catalysts are shown in Fig. 13. For all the catalysts, the desorption of N_2O and N_2 was not observed, and only the desorption peak of oxygen ($\text{m/e} = 32$) was detected. During the adsorption of N_2O at 50 $^{\circ}\text{C}$, the peak of nitrogen ($\text{m/e} = 28$) was observed. This result means that N_2O in contact with the catalyst at 50 $^{\circ}\text{C}$ is spontaneously decomposed, releasing the N_2 molecule to the gas phase and leaving the oxygen atom on the catalyst surface. For the undoped Co_3O_4 catalyst, the low-temperature peak was not observed. This result suggests that the desorption peak at 70–200 $^{\circ}\text{C}$ observed when molecular oxygen was adsorbed is due to the desorption of the molecular oxygen [32]. For the K-doped Co_3O_4 catalyst with K/Co molar ratio of 0.01, 0.02 and 0.05, the broad desorption peak of oxygen was observed at

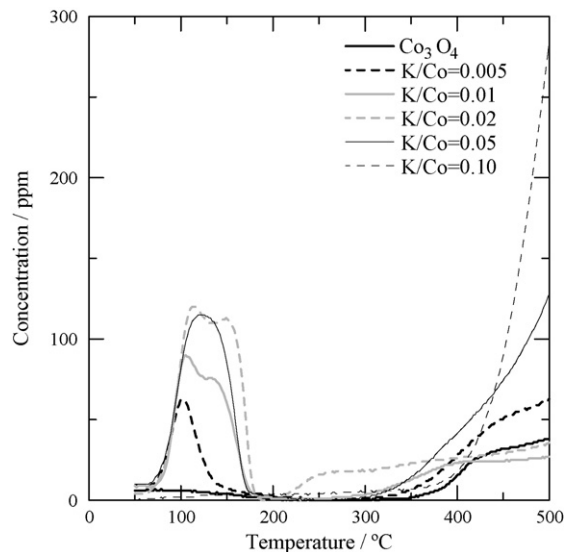
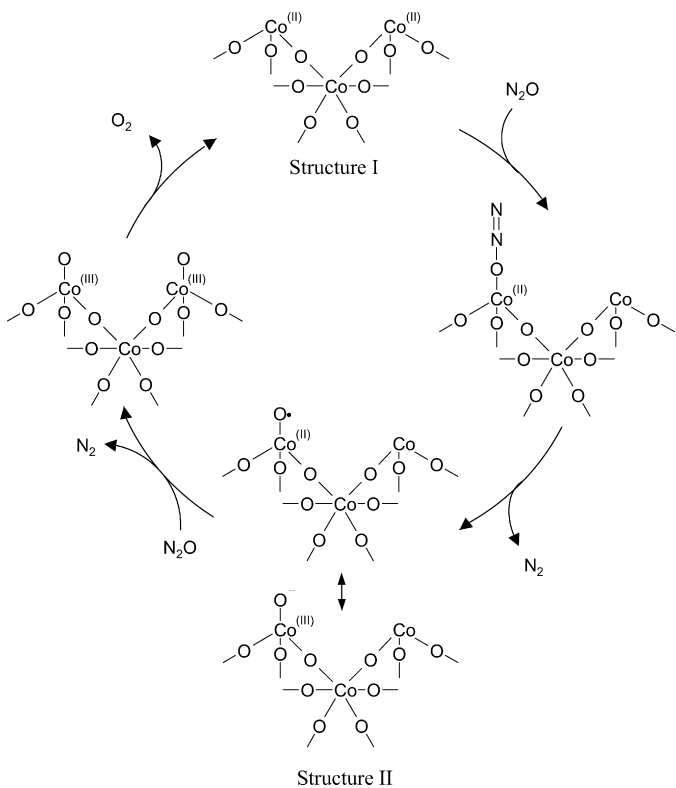


Fig. 13. TPD profiles of $\text{O}_2(\text{m/e}=32)$ after adsorption of N_2O on K-doped Co_3O_4 catalysts.



Scheme 1. Redox mechanism for N_2O decomposition on K-doped Co_3O_4 catalyst.

around 70–180 °C, and the peak profiles were essentially identical with those observed in O_2 -TPD. This result indicates that the K-doped Co_3O_4 catalysts have an ability to adsorb molecular oxygen dissociatively. For the K-doped Co_3O_4 catalyst with K/Co molar ratio of 0.10, the desorption peak was not observed, indicating that this catalyst has a low activity at 50 °C for the dissociation of the N–O bond of N_2O .

From the result obtained thus far, a redox mechanism as depicted in Scheme 1 is proposed. N_2O can be adsorbed either through oxygen or nitrogen atom [33–36]. Coordination of N_2O to acid site through the oxygen atom increases the bond order between two nitrogen atoms and decreases the bond order between nitrogen and oxygen atoms. On the other hand, coordination of N_2O through the nitrogen atom would result in an increase in the N–O order while decreasing the N–N band order. Therefore, the latter surface species would give undesirable byproducts such as NO and NO_2 . In this study, however, these products were not detected; therefore, only the former surface species was considered. Structure I is the model of the surface of the K-doped catalyst in which coordinately unsaturated Co^{II} ions are the active sites. Electron donation from the highly basic oxygen to the Co species stabilizes Structure I and increases the number of the active sites. Both oxygen and N_2O molecules are adsorbed on the active sites but the former molecule requires two vacant sites. Adsorption of N_2O on the active sites spontaneously break down the N–O bond releasing the N_2 molecule to the gas phase and remaining the oxygen atom on the active site (Structure II). This structure may be considered as Co^{III} species with surface oxide anion.

Electron donating effect of the highly basic oxygen influenced by K^+ destabilizes Structure II, thus promoting the desorption of oxygen molecule. Similar redox-based mechanism has been proposed for N_2O decomposition on various catalysts [37–44]. Interestingly, Nishiyama and co-workers [37,38] found that alkali addition to the cobalt catalyst supported on zeolites effectively promoted the catalyst activity for partial oxidation of benzyl alcohol and concluded that alkali component facilitated the oxidation of Co^{2+} to Co^{3+} to form Co_3O_4 , which is completely opposite direction of the alkali effect found in this paper. However, their reaction is an oxidation, while the present reaction is the reduction of N_2O to N_2 . Dissociative adsorption of molecular oxygen on the alkali-promoted cobalt catalyst as verified in this paper can facilitate the oxidation of Co^{2+} to Co^{3+} as proposed by Nishiyama and co-workers [37,38].

4. Conclusions

The K-doped Co_3O_4 catalyst showed high activities for the decomposition of N_2O and the activity was maintained at least for 12 h even in the presence of oxygen and water in the feed gas. The activity of the K-doped Co_3O_4 catalyst strongly depended on the amount of K in the catalyst, indicating that the interaction between K and Co_3O_4 plays an important role on the catalyst activity. The XPS, TPR and TPD measurements revealed that the number of active sites increased and desorption of oxygen was promoted by the addition of K to the Co_3O_4 catalyst. From these results a redox type mechanism was proposed in which coordinately unsaturated Co^{2+} species was stabilized by the electron donating effect of highly basic oxygen influenced by K^+ ions while Co^{3+} species (Structure II) formed by oxidation of Co^{2+} with oxygen atoms derived by N_2O decomposition was destabilized. The K-doped Co_3O_4 catalyst will have practical use for the direct decomposition of N_2O from anthropogenic source such as the nitric acid plant.

References

- [1] Third Assessment Report of the IPCC, 2001.
- [2] F. Kapteijn, J. Rodriguez-Mirasol, J.A. Moulijn, Appl. Catal. B: Environ. 9 (1996) 25.
- [3] G. Centi, A. Galli, B. Montanari, S. Perathoner, A. Vaccari, Catal. Today 35 (1997) 113.
- [4] K. Yuzaki, T. Yarimizu, K. Aoyagi, S. Ito, K. Kunimori, Catal. Today 45 (1998) 129.
- [5] J. Haber, T. Machej, J. Janes, M. Nattich, Catal. Today 90 (2004) 15.
- [6] A. Satsuma, H. Maeshima, K. Watanabe, K. Suzuki, T. Hattori, Catal. Today 63 (2000) 347.
- [7] R. Drago, K. Jurczyk, N. Kob, Appl. Catal. B: Environ. 13 (1997) 69.
- [8] S. Kannan, C.S. Swamy, Catal. Today 53 (1999) 725.
- [9] J.N. Armor, T.A. Braymer, T.S. Farris, Y. Li, F.P. Petrocelli, E.L. Weist, S. Kannan, C.S. Swamy, Appl. Catal. B: Environ. 7 (1996) 397.
- [10] U. Chellam, Z.P. Xu, H.C. Zeng, Chem. Mater. 12 (2000) 650.
- [11] J. Pieterse, S. Booneveld, R. Brink, Appl. Catal. B: Environ. 51 (2004) 215.
- [12] J. Perez-Ramirez, F. Kapteijn, G. Mul, J.A. Moulijn, Chem. Commun. 8 (2001) 693.
- [13] R.S. da Cruz, A.J.S. Mascarenhas, H.M.C. Andrade, Appl. Catal. B: Environ. 18 (1998) 223.

[14] V.K. Tzitzios, V. Georgakilas, *Chemosphere* 59 (2005) 887.

[15] C. Ohnishi, K. Asano, S. Iwamoto, K. Chikama, M. Inoue, *Catal. Today* 120 (2007) 145.

[16] C. Ohnishi, K. Asano, S. Iwamoto, M. Inoue, *Stud. Surf. Sci. Catal.* 162 (2006) 737.

[17] P.W. Park, J.K. Kil, H.H. Kung, M.C. Kung, *Catal. Today* 42 (1998) 51.

[18] M. Haneda, Y. Kintaichi, N. Bion, H. Hamada, *Appl. Catal. B: Environ.* 46 (2003) 473.

[19] S. Imamura, N. Okamoto, Y. Saito, T. Ito, H. Jindai, *Jpn. Petrol. Inst.* 39 (1996) 350.

[20] G. Centi, L. Dall’Olio, S. Perathoner, *Catal. Lett.* 67 (2000) 107.

[21] J.M. Jimenez Mateos, J. Morales, J.L. Tirado, *Thermochim. Acta* 133 (1988) 257.

[22] A. Lundblad, B. Bergman, *Solid State Ionics* 96 (1997) 173.

[23] J.C. Dupin, D. Gonbeau, P. Vinatier, A. Levasseur, *Phys. Chem. Chem. Phys.* 2 (2000) 1319.

[24] M. Haneda, I. Nakamura, T. Fujitani, H. Hamada, *Catal. Surv. Asia* 9 (2005) 207.

[25] A. Miyakoshi, A. Ueno, M. Ichikawa, *Appl. Catal. A: Gen.* 219 (2001) 249.

[26] A. Caballero, J.P. Espinós, A. Fernández, L. Soriano, A.R. González-Elipe, *Surf. Sci.* 364 (1996) 253.

[27] M. Huhler, R. Schlägl, G. Ertl, *J. Catal.* 138 (1992) 413.

[28] P. Arnoldy, J.A. Moulijn, *J. Catal.* 93 (1985) 38.

[29] M. Voß, D. Borgmann, G. Wedler, *J. Catal.* 212 (2002) 10.

[30] B.A. Sexton, A.E. Hughes, T.W. Turney, *J. Catal.* 97 (1986) 390.

[31] E. van Steen, G.S. Sewell, R.A. Makhothe, C. Micklithwaite, H. Manstein, M. de Lange, C.T. O’Connor, *J. Catal.* 162 (1996) 220.

[32] Y. Takita, T. Tashiro, Y. Saito, F. Hori, *J. Catal.* 97 (1986) 25.

[33] G. Hussain, M.M. Rahman, N. Sheppard, *Spectrochim. Acta* 47A (1991) 1525.

[34] C. Morterra, F. Bocuzzi, S. Coluccia, G. Ghiotti, *J. Catal.* 65 (1980) 231.

[35] E. Garrone, P. Ugliengo, G. Ghiotti, E. Borello, V.R. Saunders, *Spectrochim. Acta* 49A (1993) 1221.

[36] T.M. Miller, V.H. Grassian, *J. Am. Chem. Soc.* 117 (1995) 10969.

[37] D. Nakashima, Y. Ichihashi, S. Nishiyama, S. Tsuruya, *J. Mol. Catal.* 259 (2006) 108.

[38] Y. Li, D. Nakashima, Y. Ichihashi, S. Nishiyama, S. Tsuruya, *Ind. Eng. Chem. Res.* 43 (2004) 6021.

[39] E. Giamello, D. Murphy, G. Magnacca, C. Morterra, Y. Shioya, T. Nomura, M. Anpo, *J. Catal.* 136 (1992) 510.

[40] A. Dandekar, M.A. Vannice, *Appl. Catal. B: Environ.* 22 (1999) 179.

[41] Z. Zhu, G.Q. Lu, Y. Zhuang, D. Shen, *Energy Fuels* 13 (1999) 763.

[42] F. Pinna, M. Scarpa, G. Strukul, E. Guglielminotti, F. Bocuzzi, M. Manzoli, *J. Catal.* 192 (2000) 158.

[43] P.E. Fanning, M.A. Vannice, *J. Catal.* 207 (2002) 166.

[44] T. Nobukawa, M. Yoshida, K. Okumura, K. Tomishige, K. Kunimori, *J. Catal.* 229 (2005) 374.